Proceedings of 5th International Symposium on
Intelligent Manufacturing Systems, May 29-31, 2006: 1141-1149

Modeling and control of a humanoid robot hand finger

Yunus Ziya Arslan

Department of Mechanical Engineering, Faculty of Engineering, Istanbul University, 34320 Avcilar, Istanbul, Turkey
e-mail: yzarslan@istanbul.edu.tr
tel: +90 212 4737070/17748, fax: +90 212 4737180

Yuksel Hacioglu

Department of Mechanical Engineering, Faculty of Engineering, Istanbul University, 34320 Avcilar, Istanbul, Turkey
e-mail: yukselh@istanbul.edu.tr
tel: +90 212 4737070/17748, fax: +90 212 4737180

Abstract

In this study, the kinematic and dynamic analysis of closing motion of the human hand finger is carried out based on an approximate model of the human hand anatomy. Then sliding mode control is applied to this hand finger model for adding the robustness feature. Because of the similarity of kinematic structures of the finger bones to each others, motion analysis of only one finger provides general evaluation of the whole human hand behavior. During the construction of the model, care was taken to insure that the bone dimensions and masses are similar to a real human hand. It is expected that this study will be useful in giving human-like qualities to robot hands.

Key words: Humanoid robot hand, sliding mode control

Paper submission area: System modeling and simulation

1. Introduction

The need for improving the dexterous robot hands and end-effectors arises from the desire for handling objects of different size and shapes like human hands. In the literature, the motion mechanism of the human hand is adopted to robot and prosthetic hand designs to mimic natural movements. Pollard and Gilbert studied to determine the appropriate tendon arrangements of the human hand for optimizing the total muscle force requirements of robot hands. It can be concluded from this study that a robot hand can have a highly similar force capability of the human hand [1]. Li et al. determined the forces produced by extrinsic muscles and intrinsic muscle groups of individual hand fingers by using two 2 dimensional biomechanical models during isometric contractions [2]. Bundoo and Park designed a biomimetic finger actuated by a type of artificial muscle constituted by Shape Memory Alloys [3]. Weghe et al. constructed an anatomically-correct testbed of the human hand to evaluate its mechanism, function and control [4]. Fukaya et al. [5] designed a new humanoid-type hand (called TUAT/Karlsruhe Humanoid Hand) with human-like manipulation abilities for adapting to the humanoid robot ARMAR [6].

Because of their simple structure, PID controllers are used widely in industrial applications. On the other hand this type of control is not efficient when there are parameter variations and external disturbances. For that reason it is important to have a robust controller. Sliding mode control, as a special class of variable structure, is preferred in robotics and in a variety class of applications due to its invariance properties. This control method has become widespread after its introduction by Utkin [7]. The basic notion of the method is to drive the system states to the so-called sliding surface and then keep the system within a neighborhood of this surface. Slotine and Sastry [8] have developed a sliding mode controller for control of time varying non-linear systems and applied this controller to a two-link manipulator, which is to handle variable loads in a flexible manufacturing system environment. Gao and Hung [9] presented a new approach, which is called reaching law method, for the design of variable structure controller for non-linear systems. The approach was applied to a two-link robot arm to demonstrate its effectiveness. Cavallo and Natale [10] proposed a control strategy based on a second order sliding manifold MIMO approach, which is used to design a robust multivariable linear controller. Six degrees of freedom manipulator was used as a test bed for experiments.

In this study, kinematic and dynamic analysis of a three degrees of freedom (DOF) finger model, which resembles the human hand, is carried out and a robust sliding mode controller is applied to this system. Trajectory of the finger model is based on the camera images of closing motion of the real human hand and joint angles are obtained using these images in a computer aided design program. Then joint torques are calculated in dynamic analysis stage.

2. Anatomy of the Human Hand

Human hand is a very articulated structure. The high functionality of the human hand is based on the higher degrees of freedom. Human hand has 23 DOF that is provided by 17 joints [11]. If three dimensional movement is taken into consideration, degrees of freedom increases to 29 because of orientation and position variation of the hand. In Figure 1, the joints of the hand can be seen.

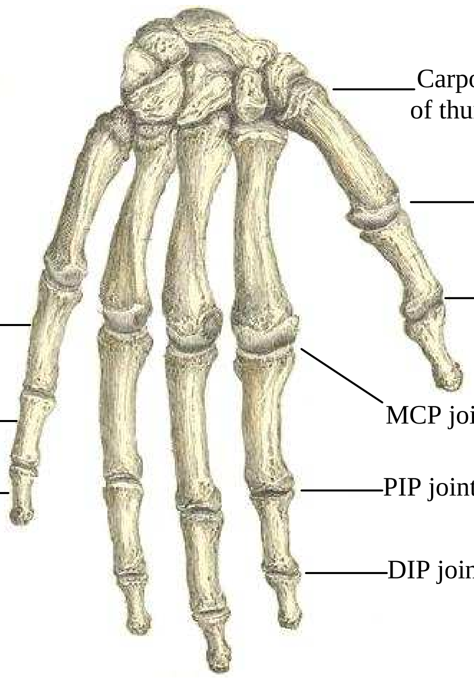

Figure 1. Joints of the human hand. *Image is adapted from [12].*

The phalanges are the small bones that constitute the skeleton of the fingers and thumb. The nearest phalange to the hand body is called “proximal” phalange and the one at the end of the each finger is called “distal” phalange. The joints of the finger, the distal interphalangeal (DIP) and proximal interphalangeal (PIP) joints, have 1 DOF owing to rotational movement and metacarpophalangeal (MCP) joint has 2 DOF owing to adduction-abduction and rotational motions. Except the thumb, the other four fingers (index, middle, ring and little fingers) have similar structure in terms of kinematics and dynamics features. Thumb is the most complex physical structure amongst the hand fingers and different from the fingers in that contains only two phalanges and has 5 DOF. The index finger has the greatest range of motion amongst the fingers such as, for the extension/flexion movement 80^o at the DIP joint, 110^o at the PIP joint and 90^o at the MCP joint. Abduction and adduction angles have been measured as 20^o at the MCP joint in the index finger [3].

3. Model of the finger

The finger model of the humanoid robot hand used in this study has three degrees of freedom. It consists of three cylindrical links, which represent the proximal, middle and distal bones of the index finger of human hand. Also there are point masses attached at the end of the each link that represent the revolute joints of the finger. The physical model of the finger is given in Figure 2.

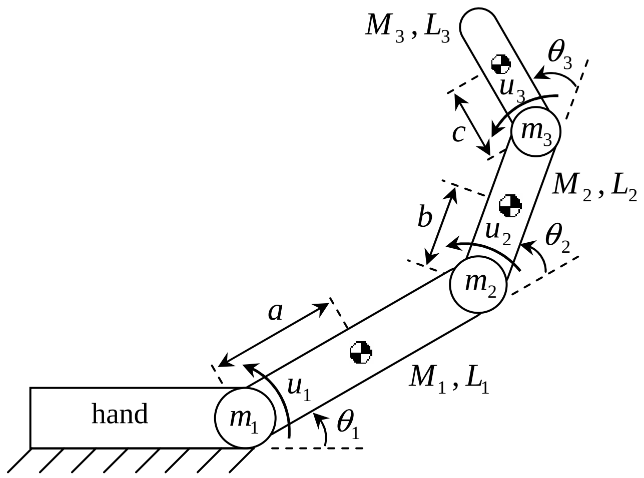

Figure 2. Finger model of the humanoid robot hand

M_i, L_i and I_i are the mass, link length and mass moment of inertia of the related links. a, b and c are the distances of the mass center of the first, second and third link, respectively. m_i represents the mass of the joints and θ_i is the joint angle of the related link.

Equations of motion are obtained by using Lagrange equations and are given in state space form as below.

$$M(\theta)\ddot{\theta} + C(\theta,\dot{\theta}) + G(\theta) = u \tag{1}$$

Here, $M(\theta)$ is $n \times n$ mass matrix of the finger, $C(\theta,\dot{\theta})$ is $n \times 1$ vector and includes the coriolis and centrifugal terms, $G(\theta)$ is $n \times 1$ vector of the gravity terms and u is $n \times 1$ generalized torque vector. For the purpose of checking the robust behavior of the controller, a resistive torque is used at the PIP joint as an unexpected joint friction fault.

4. Sliding mode control

In sliding mode controlled systems, control action is deliberately changed during control process according to certain predefined rules, which depend on the error states of the system. Then, the system moves on stable and unstable trajectories and reaches the sliding surface and error states go to zero by sliding on this surface.

The state space form of a non-linear dynamic system can be written as

$$\dot{\boldsymbol{x}} = \boldsymbol{f}(x) + [B]\,\boldsymbol{u} \tag{2}$$

For a control system, the sliding surface can be selected as

$$\boldsymbol{\sigma} = [G]\,\boldsymbol{\Delta x} \tag{3}$$

Here $\mathbf{\Delta x} = \mathbf{x_r} - \mathbf{x}$ is the difference between the reference value and system response. $[G]$ includes the sliding surface slopes. Then:

$$\sigma_i = \alpha_i \, e_i + \dot{e}_i \tag{4}$$

α_i represents the negative value of the each related sliding surface slope. For stability, the following Lyapunov function candidate, which is proposed for a non-chattering action, has to be positive definite and its derivative has to be negative semi-definite.

$$\boldsymbol{v}(\boldsymbol{\sigma}) = \frac{\boldsymbol{\sigma}^T \boldsymbol{\sigma}}{2} > 0 \tag{5}$$

$$\frac{d\,\mathbf{v}(\boldsymbol{\sigma})}{dt} = \frac{\dot{\boldsymbol{\sigma}}^T \boldsymbol{\sigma}}{2} + \frac{\boldsymbol{\sigma}^T \dot{\boldsymbol{\sigma}}}{2} \le 0 \tag{6}$$

If the limit condition is applied to equation (6), and from equation (2) and equation (3) the controller force for the limit case is obtained:

$$\boldsymbol{u}_{eq} = [GB]^{-1} \left(\frac{d\boldsymbol{\Phi}(t)}{dt} - [G]\, \boldsymbol{f}(x) \right) \tag{7}$$

Equivalent control is valid only on the sliding surface. So an additional term should be defined to pull the system to the surface. For this purpose derivative of the Lyapunov function can be selected as follows.

$$\dot{\boldsymbol{v}} = -\boldsymbol{\sigma}^T [\varGamma] \boldsymbol{\sigma} < 0 \tag{8}$$

By carrying out necessary calculations, total control input is found as

$$\boldsymbol{u} = \boldsymbol{u}_{eq} + [GB]^{-1} [\Gamma]\, \boldsymbol{\sigma} \tag{9}$$

$[GB]^{-1}$ is always pseudo-inverse and equal to mass matrix for mechanical systems. $[\Gamma]$ is a positive definite matrix, and value of terms are decided by trial at the design stage. However, if the knowledge of $\boldsymbol{f}(x)$ and $[B]$ are not well known, the calculated equivalent control inputs will be completely different from the needed equivalent control inputs. Thus, in this study, it is assumed that the equivalent control is the average of the total control. For estimation of the equivalent control, an averaging filter, here a low pass filter, can be designed as follows.

$$\hat{\boldsymbol{u}}_{eq} = \frac{1}{\tau s + 1} \boldsymbol{u} \tag{10}$$

Finally the non-chattering control input is defined as

$$\boldsymbol{u} = \hat{\boldsymbol{u}}_{eq} + [GB]^{-1} [\Gamma]\, \boldsymbol{\sigma} \tag{11}$$

5. Trajectory planning and numerical results

Trajectory planning is an important stage in the robot finger model design since the humanoid robot is hoped to simulate the natural movements of the human finger. In this study, the flexion movement of the index finger of human hand is investigated. For this purpose the movement of human hand while fingers are closing down was recorded by using a digital camera. The recorded video was split into frames with 0.08 second time intervals. Then these frames were transferred into a computer aided design program where the joint angles were measured with the aid of the marks, which are placed on the finger joints in the beginning.

In order to have continuous reference paths for the joint angles, sixth order polynomials were fitted to the experimental data. The experimental data and their polynomial approximations are given in Figure 3 (a,b,c). By using the polynomials as reference, the motion of the end of the distal link is obtained as given in Figure 3.d. It is seen from this figure that the obtained trajectory is a natural one. Thus the obtained polynomials will be used as reference for the sliding mode controller through the numerical analysis of the finger model.

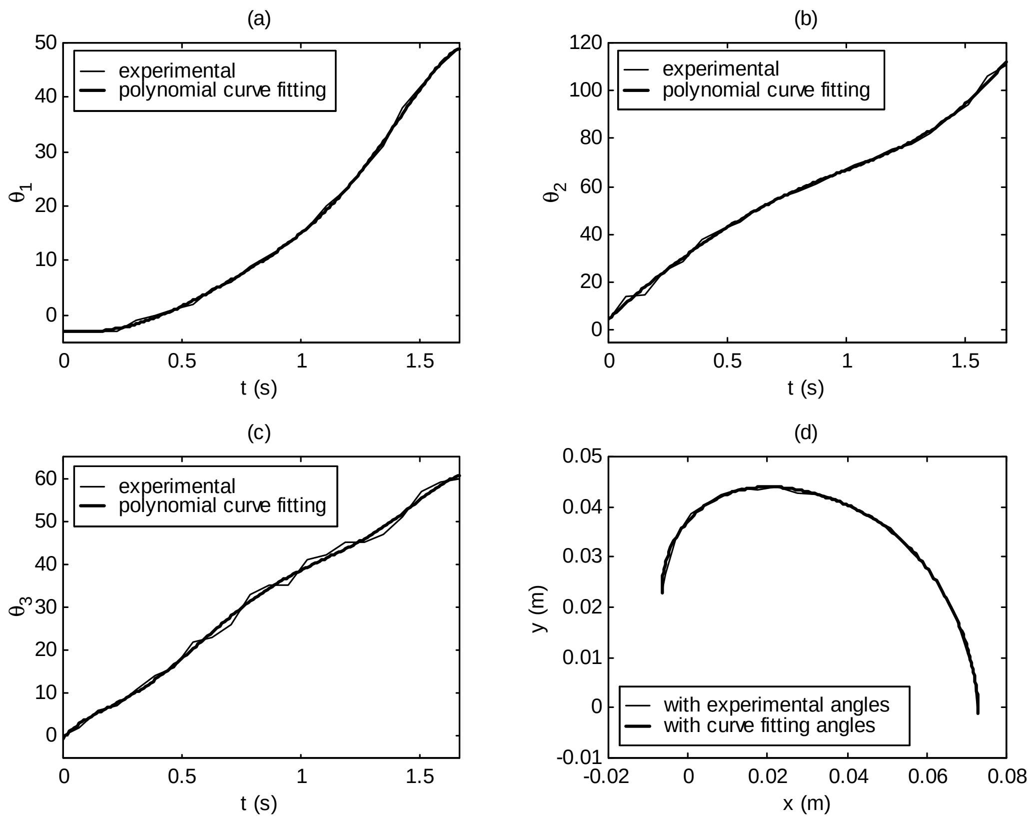

Figure 3. (a, b, c) Experimental data of joint angles and their polynomial approximations. d) Trajectory of the robot hand

It should be noted that during simulations an unexpected joint friction fault occurs after the 0.3rd second, which tests the robust behavior of the controller. This resistive friction is shown in Figure 4.

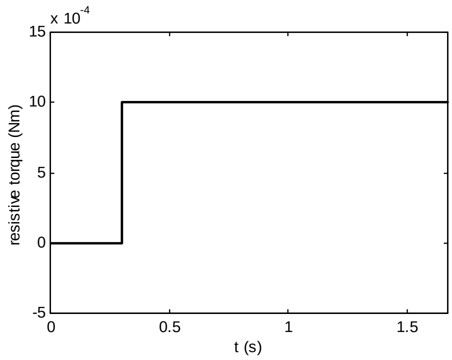

Figure 4. Applied resistive torque to the PIP joint

In Figure 5, the references for the joint angles and tracking errors for the related links are given. It is seen from this figure that the each link of the finger tracks the specified trajectory successfully in spite of the unexpected joint friction fault, which indicates the efficiency and robust behavior of the sliding mode controller.

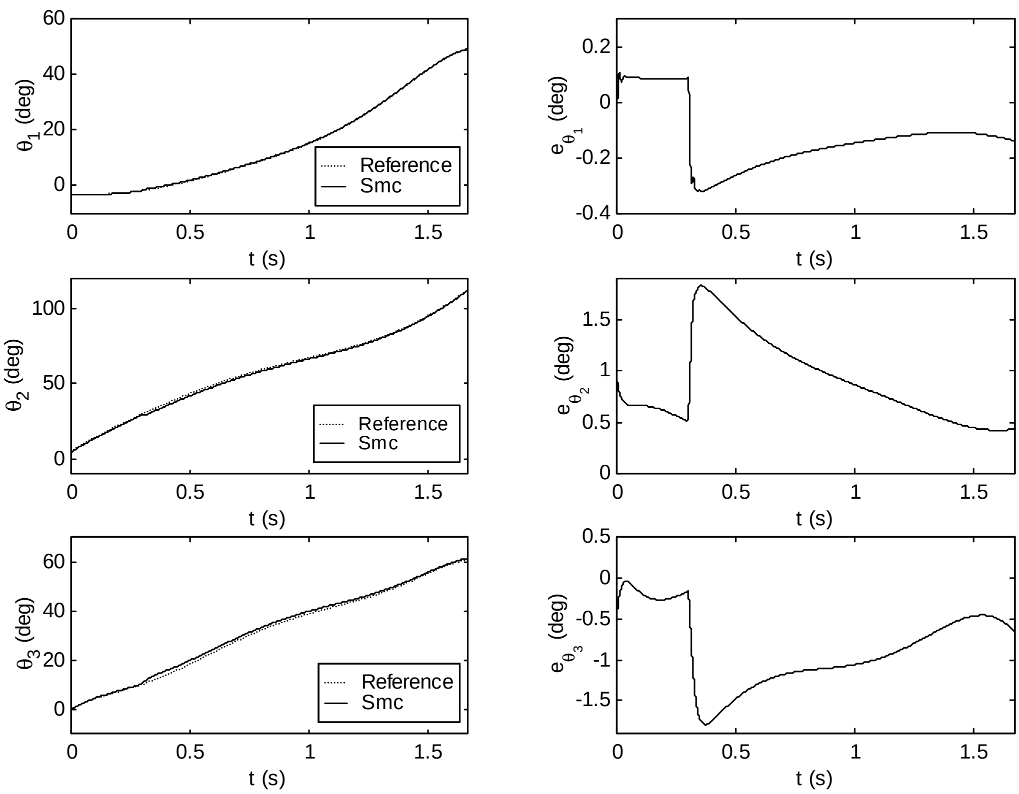

(a) (b)

Figure 5. a) Reference and actual values for joint angles b) Tracking errors for the links

The generalized torque of each link is given in Figure 6. Generalized torques are the output signals of the controller, and are used to manipulate the finger. Maximum joint torque is obtained for the MCP joint and the minimum force was obtained for the DIP joint, which is also expected.

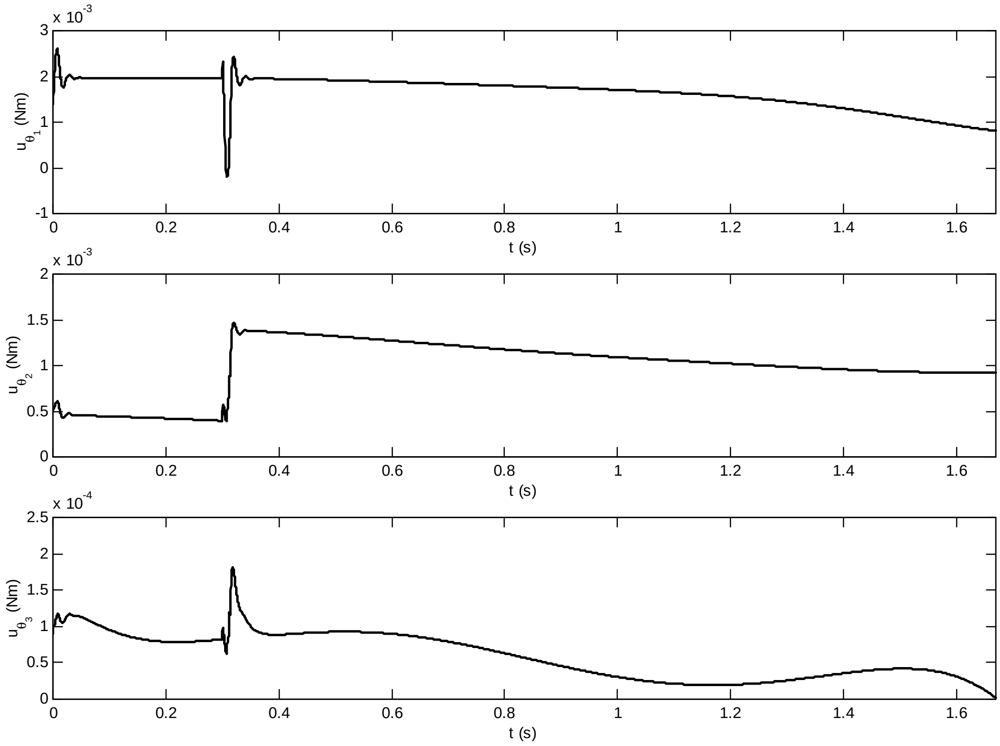

Figure 6. Generalized torques produced by sliding mode controller.

6. Conclusion

In this study, humanoid robot finger model was presented. The model was designed with respect to index finger of the human hand. First, path of the end point of the finger was determined using camera images during the closing motion of the human hand and, then joint angles were obtained with the aid of a computer aided design program. Second, in dynamic analysis of the finger model, joint torques was acquired. Then, sliding mode controller was applied to the system. From the numerical results it can be concluded that by using the sliding mode controller an efficient tracking performance was obtained despite the unexpected friction fault. Additionally, the results have shown that the presented control method can be used in humanoid robot hand studies in order to improve the life conditions of handicapped people.

References

[1] Pollard, N., Gilbert, R.C., “Tendon Arrangement and Muscle Force Requirements for Humanlike Force Capabilities in a Robotic Finger”, Proceedings of the IEEE International Conference on Robotics and Automation (ICRA '02), May, 2002.

[2] Li, Z.M, Zatsiorsky, V.M, Latash, M.L., “The effect of extensor mechanism on finger flexor force”, 24th Annual Meeting of the American Society of Biomechanics, University of Illinois at Chicago, July 19-22, 2000.

[3] Bundhoo, V., Park, E. J., “Design of an Artificial Muscle Actuated Finger towards Biomimetic Prosthetic Hands”, 12th International Conference on Advanced Robotics ICAR Seatle, 2005.

[4] Weghe, M.V., Rogers, M., Weissert, M., Matsuoka, Y., “The ACT hand: Design of the skeletal structure”, Proceedings of the 2004 IEEE International Conference on Robotics, LA, April 2004, 3375-3379.

[5] Fukaya, N., Toyama, S., Asfour, T., Dillmann, R., “Design of the TUAT/Karlsruhe Humanoid Hand”, IEEE/RSJ International Conference on Intelligent Robots and Systems (IROS2000), Takamatsu, Japan, October 30 - November 5, 2000

[6] Asfour, T., Berns, K., Dillmann, R., “The Humanoid Robot ARMAR”, Proc. of the Second International Symposium on Humanoid Robots (HURO´99), October 8-9, 1999, Tokyo, Japan.

[7] V.I. Utkin, “Variable structure systems with sliding modes”, IEEE Transactions on Automatic Control 22 (1977), 212-222.

[8] Slotine J.J., Sastry, S.S., “Tracking control of nonlinear systems using sliding surfaces, with application to robot manipulators”, International Journal of Control 38(2) (1983), 465-492.

[9] Gao, W., Hung, J.C., “Variable structure control of nonlinear systems: A new approach”, IEEE Transactions on Industrial Electronics 40(1) (1993), 45-55.

[10] Cavallo, A., Natale, C., “High-order sliding control of mechanical systems: theory and experiments”, Control Engineering Practice 12 (2004), 1139-1149.

[11] Joseph J. LaViola, Jr., “A survey of hand posture and gesture recognition techniques and technology ” Technical Report CS-99-11, Department of Computer Science, Brown University, June 1999.

[12] http://www.anatomyatlases.org/atlasofanatomy/plate05/12rhanddorsal.shtml (access time: 24.02.2006)